

Uncovering Hydrocarbon Potential Using the Integration of Simultaneous Seismic Inversion and Rock Physics at the “NS” Field, Kutai Basin, Kalimantan

Nine Safira^{1*}, Haryono², Agus Riyanto¹, Hotma Yusuf²

¹Geophysics Study Program, Geoscience Department, Faculty of Mathematics and Natural Sciences,
University of Indonesia, Depok, 16424, Indonesia

²Saka Energi Indonesia

*Corresponding author's email: nine.safira@sci.ui.ac.id

Abstract. Reservoir characterization is a series of stages of evaluating, analyzing, and interpreting reservoir conditions. One method for complete reservoir characterization is the simultaneous seismic inversion method. A seismic inversion method using pre-stack data integrates several angles of incidence with wavelet associations at each angle and integrates well data. The implementation of this method can produce several rock physics properties such as P-wave velocity (V_p), S-wave velocity (V_s), density, V_p/V_s ratio, and P-wave acoustic impedance (Z_p), and S-wave acoustic impedance (Z_s). In addition, Lambda-Mu-Rho and scaled-Qp (SQp) and scaled-Qs (SQs) transformations were also applied as the outputs of further rock physics models. The advantages of this transformation are the accuracy in lithological discrimination and the better type of pore fluid in the hydrocarbon reservoir. In addition, AVO modeling as AVO class classification and fluid substitution modeling simulation (FRM) was carried out. This study analyzes hydrocarbons' potential using simultaneous seismic inversion, elastic impedance inversion, and rock physics modeling in the "NS" Field, Kutai Basin, Kalimantan. The results of this study are lateral distributions indicating the presence of gaseous hydrocarbon prospects, characterized by the definition of properties Z_p , density, Lambda-Rho, Poisson ratio, and SQp with relatively low values, and properties of Z_s , Mu-Rho, and SQs with relatively high values. In addition, the results of the AVO classification indicate that the gas reservoir is classified as class III with a positive AVO product value. The hydrocarbon zoning weighting was then carried out to see the zones with the highest to lowest hydrocarbon indications in the 4 Ma Formation and 7.6 Ma Formation.

Keywords: Simultaneous Seismic Inversion, Reservoir Characterization, AVO, Kutai Basin, Gas Hydrocarbons.

1. Introduction

Acoustic impedance (AI) is often used to extract specific information about the physical properties of rocks. However, the results of the post-stack acoustic impedance inversion have not been able to provide good discrimination regarding the porosity between carbonate lithology and claystone¹. Therefore, simultaneous seismic inversion was developed to extract rock property information from seismic data to provide solutions to geological problems that cannot be solved only by performing post-stack² acoustic impedance inversion. In addition to simultaneous seismic inversion, elastic impedance inversion can combine pre-stack seismic data with well data based on the angle formed from the incident wave, namely 10 degrees, 20 degrees, and 30 degrees³.

The results of simultaneous seismic inversion are extracted to produce a combination of other rock properties. Some of them are Lamé parameter transformations, namely Lambda-Rho and Mu-Rho⁴ and scaled inverse-Qp (SQp) and scaled inverse-Qs (SQs) transformations developed by Hermana, Ghosh, and Sum⁵. Amplitude versus Offset analysis methods and Fluid Substitution Modeling (FRM) are used to validate the presence of gaseous hydrocarbon indications.

This research focuses on gas hydrocarbon reservoirs in the "NS" Field, Kutai Basin, Kalimantan. The field is a gas producer in the reservoir range of the 4 Ma Formation to 7.6 Ma Formation, which is included in the Kampung Baru Formation to the Balikpapan Formation. Integrated analysis of the combined rock properties resulting from simultaneous seismic inversion and inversion of elastic impedance accompanied by validation of AVO analysis and fluid substitution modeling is expected to reduce uncertainty and provide results with a high level of accuracy regarding the hydrocarbon indication zone in the research area coverage.

2. Data and Methodology

In carrying out this research, it is necessary to prepare the primary and supporting data. The main data includes 3D partial angle stack seismic data and well log data. In addition, the supporting data to help the primary data processing includes checkshot data, marker data, and speed data. The inventory of the main and supporting data can be seen in **Table 1**.

Table 1. Research data inventory

No	Data Subject	Format	Quantity
1	3D Seismic Partial Angle-stack	.segy	3
2	Well Log	.LAS / .txt	3
3	Checkshot	.xlsx	3
4	Well Marker	.xlsx	1 set

The 3D partial angle stack seismic data used in this study includes three angles: near angles with values of 0 to 10 degrees, mid angles with values of 10 to 20 degrees, and far angles of 20 to 30 degrees. The volume of seismic data and the base map of the research area can be seen in **Figure 2**.

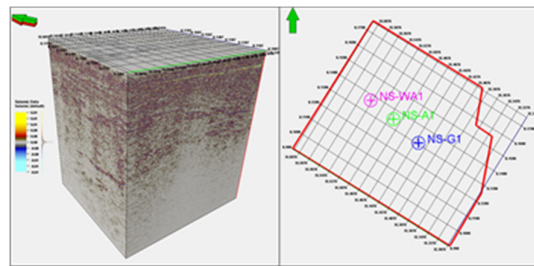


Figure 2. Seismic volume (left) and basemap of seismic data coverage and well data (right) of the study area

The well log data in this study includes three wells, namely the NS-WA1 Well, the NS-A1 Well, and the NS-G1 Well. Based on the position of the three wells in the seismic data used in this study, the NS-WA1 well is at inline 1460 and crossline 5506, well NS-A1 is at inline 1438 and crossline 5006, well NS-G1 is at inline 1397 and crossline 4424. wells include Gamma Ray, Caliper, Resistivity, Neutron Porosity, Density, DT (Sonic) log data, SDT, PHIE, PHIT, Vshale, and Sw.

In general, the research flow chart can be seen in Figure 3. The research stage begins with seismic conditioning data and well data. All seismic data volumes were matched for inline and crossline ranges, namely in the inline range 990-1846 and crossline 3076-6176. On the other hand, the well data conditioning step includes a sensitivity test. The sensitivity test is divided into several categories, namely cross plots between rock properties of P-wave velocity (V_p) and S-wave velocity (V_s), P-wave acoustic impedance log ($\ln(Z_p)$), and S-wave acoustic impedance log ($\ln(Z_s)$), P-wave acoustic impedance (Z_p) with ratio V_p and V_s , scaled- Q_s with S-wave velocity (V_s). Color indicators in the cross-plot process include clay volume (Vshale) and water saturation (Sw). Furthermore, a well to seismic tie process is carried out to establish a correlation between the well data and seismic data.

The picking horizon and fault stages are the first stages in seismic data interpretation. Horizon picking was carried out on the Seabed, the top of the 4 Ma Formation, and the top of the 7.6 Ma Formation. Furthermore, fluid substitution (FRM) modeling was carried out in the three research wells with a reservoir scenario of 100% filled with gas, water, or oil. The next stage is AVO modeling and analysis. At this stage, a comparison is made between the synthetic seismic data and the original seismic data regarding the response of changes in amplitude to changes in offset. After the conditioning process and sensitivity test indicate the presence of the prospect area, the research can proceed to the simultaneous seismic inversion stage. The resulting description of each property is in the form of distribution values of P-wave acoustic impedance (Z_p), S-wave acoustic impedance (Z_s), P-wave velocity (V_p), and S-wave velocity (V_s), and density. After the physical properties of the rock resulting from the simultaneous seismic inversion have been formed, the research continues towards the stages of Lambda-Mu-Rho (LMR), Scaled- Q_p (SQp), and Scaled- Q_s (SQs) transformations, and Poisson's ratios.

One of the additional methods in this research is the post-stack partial angle inversion to get the value of the elastic impedance. By analyzing the distribution of elastic impedance rock properties, it is possible to determine the impedance effect of each independent angle or angle of incidence on 3D partial angle stack seismic data. Then, the distribution was carried out laterally on the top of the 4 Ma Formation, the top of the 7.6 Ma Formation, between the 4 to 7.6 Ma Formation, and between the 7.6 Ma Formation to a depth of 1500 ms. The lateral distribution aims to see the distribution of rock property responses from each data processing result so that interpretations can be made regarding the potential gas reservoir zone in the research area. The final stage includes weighting the hydrocarbon zones from each rock property analysis resulting from data processing in the 4 Ma Formation and 7.6 Ma Formation.

The interpretation of one rock property is given a multiplier factor of one, the interpretation of integration is assigned a multiplier of two, and the AVO analysis is given a multiplier of three. The formula for weighting the hydrocarbon zone can be seen as follows:

$$\begin{aligned} \text{Zona Prospek HC 4 Ma} = & 1 * (Zp + Zs + Vp + Vs + Dn + LR + MR + SQp + SQs + EI) * 1 \\ & + 2 * (VpVs + \ln Zp \ln Zs + SQsVs + EI1030) + 3 * (EIAVO + AVO) \end{aligned} \quad (1)$$

$$\begin{aligned} \text{Zona Prospek HC 7.6 Ma} = & 1 * (Zp + Zs + Vp + Vs + Dn + LR + MR + SQp + SQs + EI) \\ & + 2 * (VpVs + \ln Zp \ln Zs + SQsVs + EI1030) + 3 * (EIAVO) \end{aligned} \quad (2)$$

Where: Zp = P-wave acoustic impedance; Zs = S-wave acoustic impedance; Vp = P-wave speed; Vs = S-wave speed; Dn = density; LR = Lambda-Rho; MR = Mu-Rho; SQp = scaled-Qp; SQs = scaled-Qs; EI = elastic impedance; $VpVs$ = P-wave speed and S-wave speed; $\ln Zp \ln Zs$ = log of P-wave acoustic impedance and log of S-wave acoustic impedance; $SQsVs$ = scaled-Qs and S-wave velocity; $EI1030$ = elastic impedance 10 degrees and elastic impedance 30 degrees; $EIAVO$ = AVO product elastic impedance; and AVO = AVO product.

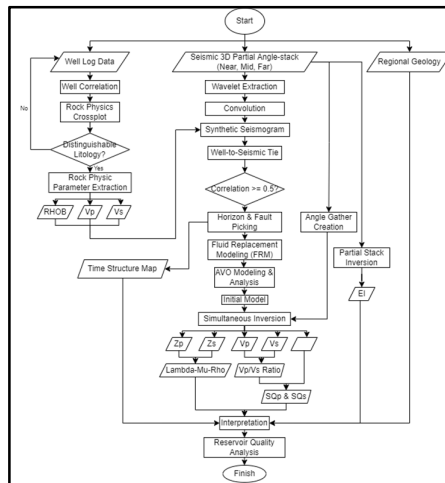


Figure 3. Research flow chart

3. Results and Discussion

After processing the data in the form of simultaneous seismic inversion and elastic impedance inversion, several selected rock properties were obtained, namely P-wave acoustic impedance (Zp), S-wave acoustic impedance (Zs), density, Lambda-Rho (LR), Mu-Rho (MR), scaled-Qp (SQp), scaled-Qs (SQs), and elastic impedance (EI) 10 degrees, 20 degrees, and 30 degrees. Based on the research results in interpreting each rock property resulting from simultaneous seismic inversion and elastic impedance, integration analysis can be carried out to provide better accuracy in delineating hydrocarbon indication zones in the study area. The integration analysis includes a combination of Vp with Vs (see Figure 4), $\ln(Zp)$ with $\ln(Zs)$ (see Figure 5), SQs with Vs (see Figure 6), and EI of the angle of incidence of 10 degrees with 30 degrees (see Figure 7). In addition, AVO analysis was carried out to validate the presence of class III gas anomalies.

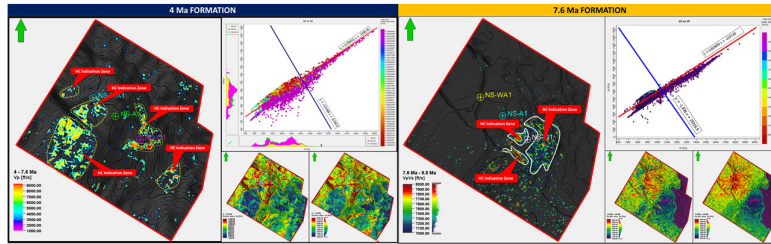


Figure 4. Interpretation between rock properties of P-wave velocity (V_p) and S-wave velocity (V_s) on a lateral map accompanied by reference cross plots of hydrocarbon zoning separation in the 4 Ma Formation (left) and the 7.6 Ma Formation (right)

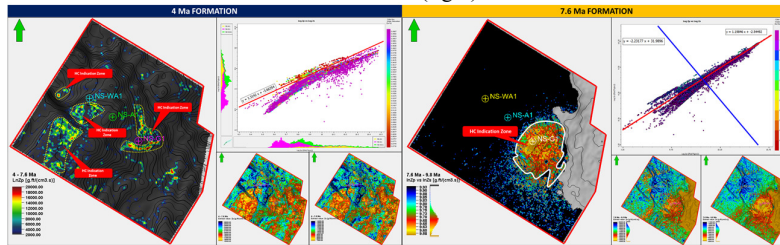


Figure 5. Interpretation between rock properties of P-wave acoustic impedance log ($\ln(Z_p)$) and S-wave acoustic impedance log ($\ln(Z_s)$) on a lateral map accompanied by a reference cross plot of hydrocarbon zoning separation in the 4 Ma Formation (left) and the 7.6 Ma Formation (right)

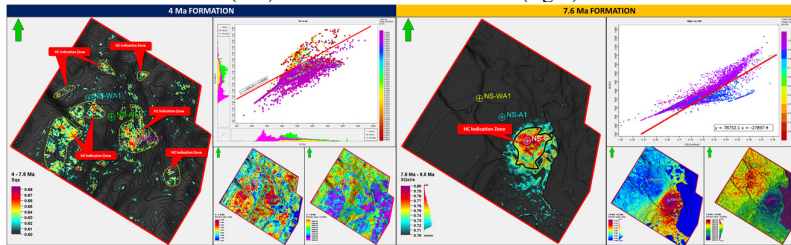


Figure 6. Interpretation between Scaled-Qs (SQ_s) rock properties with S-wave velocity (V_s) on a lateral map accompanied by a reference cross plot of hydrocarbon zoning separation in the 4 Ma Formation (left) and the 7.6 Ma Formation (right)

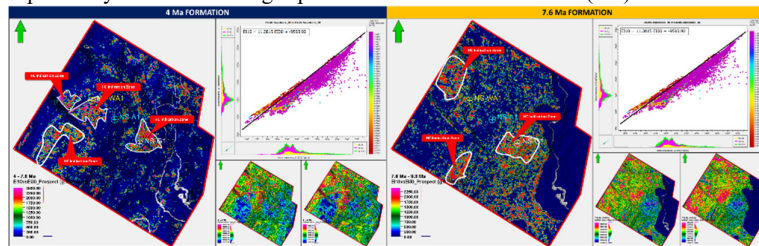


Figure 7. Interpretation between the elastic impedance (EI) rock property of a 10-degree angle of incidence with an elastic impedance (EI) of a 30-degree angle of incidence on a lateral map accompanied by a cross plot of reference for the separation of hydrocarbon zoning in the 4 Ma Formation (left) and the 7.6 Ma Formation (right)

The 4 Ma Formation shows hydrocarbon indication zones in the depth range of 820 ms to 840 ms and 900 ms to 1010 ms. The 7.6 Ma Formation shows indications in the depth range of 1000 ms to 1290 ms. The low Z_p value response can identify the presence of gas. This refers to the condition of the gas filling the rock pores, which will cause the rock to become more compressed. The response value of Z_s tends to be low but will maintain its weight more if there is a hydrocarbon anomaly. A low V_p value indicates the presence of hydrocarbons, and V_s tends to be higher. Furthermore, the rock density property has a low value because rocks containing gas will have a lower density value when compared to rocks without any hydrocarbon content. In addition, the Lambda-Rho value response has a value that tends to be lower when compared to the Mu-Rho value response. The SQ_p response is similar to Gamma Ray (GR) log data⁵. Therefore, these attributes can be used as lithology determinants. Low SQ_p values indicate indications of hydrocarbon anomalies. The response value of SQ_s , which suggests the presence of hydrocarbons, is characterized by a high value.

In addition to the interpretation and integration of rock properties resulting from simultaneous seismic inversion and elastic impedance inversion, analysis and interpretation are also carried out on

the volume of AVO products. The research focuses more on determining the bright spot of AVO product attributes in the 4 Ma Formation. Referring to the interpretation results in **Figure 8**, there are three bright spot zones in the research area. Zones 1 and 2 are strongly indicated as gas sand reservoirs with negative I and G values at the top of the reservoir accompanied by positive I and G values at the base reservoir.

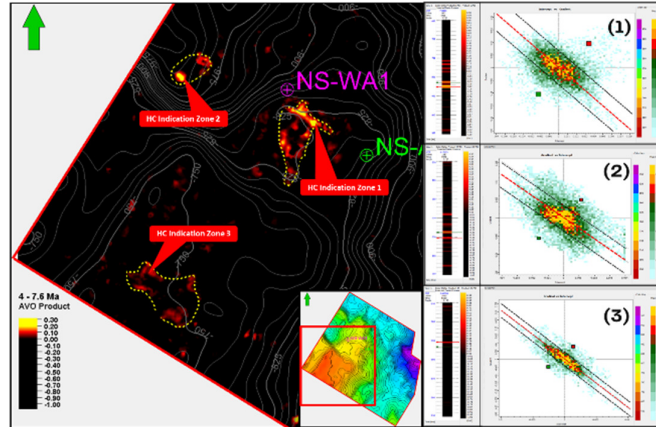


Figure 8. Interpretation results on the lateral distribution map for AVO products accompanied by validation of AVO picking in each hydrocarbon indication zone in the 4 Ma Formation coverage

The lateral distribution map resulting from the weighting of the hydrocarbon zones in the 4 Ma Formation and 7.6 Ma Formation can be seen in **Figure 9**. Areas with a color range getting closer to red will indicate a higher level of hydrocarbon prospects. Therefore, it is necessary to calculate the area and indication level of each hydrocarbon prospect zone. The distribution of these values can be seen in **table 2**.

Table 2. Distribution of area and level of hydrocarbon prospect zones in the 4 Ma and 7.6 Ma Formation

4 Ma Formation		7.6 Ma Formation	
HC Zone	Indication Level [%]	HC Zone	Indication Level [%]
1	97	1	95
2	78	2	65
3	40	3	30
4	35	4	20
5	30		
6	15		

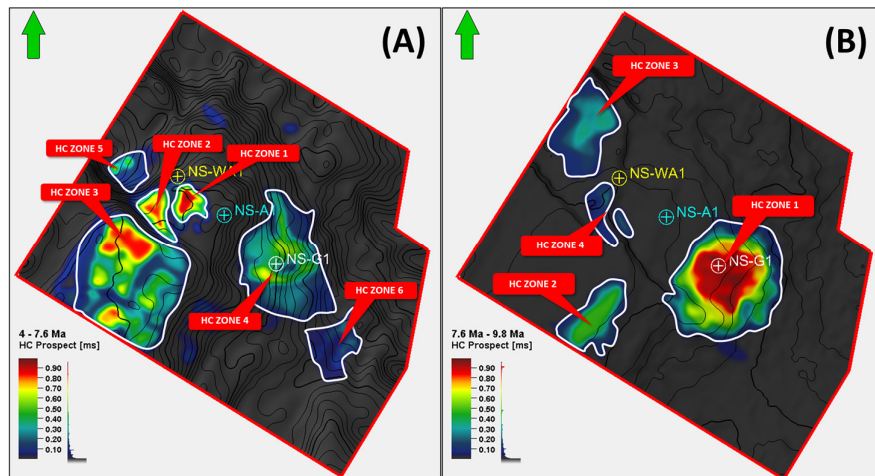


Figure 9. Weighted lateral distribution map showing hydrocarbon indication zones in: (a) 4 Ma Formation, and (b) 7.6 Ma Formation

The research area is located at the bottom of the Kutai Basin with the southern boundary in the form of the Adang Fault. The research area is east of the Sepinggan delta lobe, with the eastern boundary being the North Makassar Basin and the Mahakam Delta open to the north. Referring to **Figure 10**, the research area's coverage coincides with the gas-producing field's location. The direction of deposition of the research area can come from two sources, namely from the southwest and northwest of the research area. The research area is located at the boundary between the Kutai Basin and the Barito Basin, namely the Adang Fault. The sediment source comes from paternoster platform debris and clastic sediments in the Sepinggan delta region.

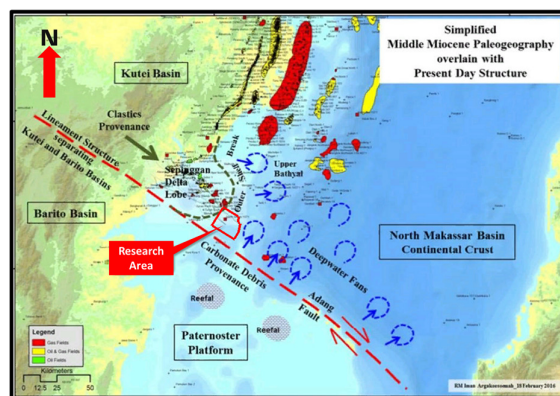


Figure 10. Location of the study area based on present structure and Middle Miocene age paleogeography (modified from Argakoesomah et al.⁶)

4. Conclusions

1. Based on the weighted distribution results in the 4 Ma Formation, six prospect zones were obtained with the order of strongest to lowest indications from HC 1 Zone, HC 2 Zone, HC Zone 3, HC Zone 4, HC Zone 5, and HC Zone 6. In the 7.6 Ma Formation, four prospect zones were obtained in order of strongest to lowest indication, namely Zone HC 1, Zone HC 2, Zone HC 3, and Zone HC 4.
2. The deposition comes from the southwest and northwest of the study area. The sediment source comes from paternoster platform debris and clastic sediments in the Sepinggan delta region.

Acknowledgments

The authors would like to thank Saka Energi Indonesia for providing the research data and technical guidance.

References

- [1] Y. Li, J. Downton and B. Goodway, "Recent applications of AVO to carbonate reservoirs in the Western Canadian Sedimentary Basin", *The Leading Edge*, vol. 22, no. 7, pp. 670-674, 2003. Available: 10.1190/1.1599694.
- [2] R. Cataldo and E. Leite, "Simultaneous prestack seismic inversion in a carbonate reservoir", *REM - International Engineering Journal*, vol. 71, no. 1, pp. 45-51, 2018. Available: 10.1590/0370-44672016710024.
- [3] P. Connolly, "Elastic impedance", *The Leading Edge*, vol. 18, no. 4, pp. 438-452, 1999. Available: 10.1190/1.1438307.
- [4] B. Goodway, T. Chen, J. Downton, "Improved AVO fluid detection and lithology discrimination using Lamé petrophysical parameters; " $\lambda\rho$ ", " $\mu\rho$ ", & " λ/μ fluid stack", from P and S inversions", *SEG Technical Program Expanded Abstracts*, pp 183-186, 1997.
- [5] M. Hermana, D. Ghosh, C. Sum, "Optimizing the Lithology and Pore Fluid Separation Using Attenuation Attributes", *The Offshore Technology Conference Asia*, 2016
- [6] R. Argakoesomah, H. Nainggolan, A. Hidayat, I. Wahyudi, M. Shahab, "Fluvial-to-Deepwater Stratigraphy and Structural Development of the Southern Part of North Makassar Basin, Indonesia", *Indonesian Petroleum Association 40th Annual Convention Proceedings*, 2016.